journal

J. Am. Ceram. Soc., 93 [11] 3757–3763 (2010)
DOI: 10.1111/j.1551-2916.2010.03976.x

DSC Method for Determining the Liquidus Temperature of Glass-Forming Systems

Eduardo Bellini Ferreira,[†,‡] Moysés L. Lima, and Edgar D. Zanotto

Vitreous Materials Laboratory—LaMaV, Department of Materials Engineering—DEMa, Univ Federal de São Carlos, São Carlos 13565-905, São Paulo, Brazil

We developed and successfully tested a differential scanning calorimetry (DSC) method to estimate the *liquidus* temperature (T_L) of good glass-forming systems, i.e., that are reluctant to crystallize. The method was first tested for several Li_2O–B_2O_3 glasses. The onset, peak, and endpoint temperatures of DSC melting peaks were measured and compared with the *liquidus* in the phase equilibrium diagram. DSC runs were carried out at different heating rates and T_L at equilibrium was estimated by extrapolation to 0°C/min. For glasses that do not crystallize during a typical DSC run, a previous heat treatment was necessary to induce crystallization. The *liquidus* of three multicomponent glasses were then obtained by DSC and compared with the T_L obtained by a direct technique using optical microscopy. The endpoint of the DSC melting peaks measured at different rates and extrapolated to 0°C/min was the best estimate for the *liquidus* of such glasses. Most results differ by not more than 10°C. Because of the small amount of glass needed, the possibility of instrumental detection, simultaneous crystallization pretreatment of many different compositions, and the speed of the DSC analysis, the proposed technique may be a valuable option to estimate the *liquidus* of simple or complex multicomponent glasses.

I. Introduction

THE *liquidus* (T_L) is the ultimate temperature of thermodynamic equilibrium between the solid and liquid phases of any material, above which crystals are unstable. This is a very important parameter in the glass industry. One must know T_L, for instance, to precisely manage the temperatures at which glass melting and forming processes can be operated. However, the accurate determination of T_L is very difficult and time consuming for glass compositions designed to resist crystallization, i.e., for most commercial compositions, because incipient crystallization must be detected.

Thermodynamic models to predict the *liquidus* of glass-forming systems have been available for some time,[1–4] although they are not practical for studying complex compositions because thermodynamic data are necessary and are often unavailable or difficult to determine. There are also empirical methods[5–8] to calculate the *liquidus* based on the chemical composition. Although thermodynamic methods sometimes yield satisfactory results, the empirical models strongly depend on the actual chemical composition and it is often not practical to extrapolate out of the range of the previous experiments.

The traditional procedure to measure the T_L of glass-forming compositions involves promoting crystallization in glass samples at temperatures close to the expected *liquidus* and making a subsequent microscopic analysis of these samples to search for crystals. The procedure can be accelerated in a gradient furnace, where a long sample or several small samples can be treated simultaneously at different temperatures. Liquid and crystals are in equilibrium at the *liquidus* and all the crystals dissolve above it after a certain time. Therefore, a microscopic (or other type of) analysis is necessary to find the transition region of the sample that still contains some crystals to that are devoid of any crystal. The corresponding temperature (i.e., the intermediary temperature between both states) is the *liquidus*. In a simple furnace, the technique follows the same criteria, but the heat treatments must be run separately for each temperature, thus requiring several treatments to cover an appropriate range of temperatures. Both techniques are time consuming, especially for the determination of the T_L of commercial glasses designed to resist crystallization, because each heat treatment takes several hours or days. Moreover, the accuracy of such techniques depends on parameters that are difficult to control, such as the variation and accuracy of the furnace temperature and the limit of resolution of the microscopic analyses.

The *liquidus* of systems that crystallize easily is generally determined with simpler procedures that accurately detect the beginning of crystallization on the heating path. Thermal analysis techniques such as differential scanning calorimetry (DSC) or differential thermal analysis (DTA) may be used for this purpose. Because of the simplicity of such techniques, they are potentially attractive for the experimental determination of the *liquidus* of complex multicomponent glasses. This possibility is the focus of this work.

A typical DSC trace for an easy-to-crystallize, stoichiometric glass shows at least three well-defined characteristic signs upon heating: the glass transition, an exothermic crystallization peak, and an endothermic melting peak (Fig. 1). However, DSC curves of complex multicomponent systems that are reluctant to crystallize (as most commercial glasses are) normally show no crystallization peak and hence no melting peak.

Systems that crystallize on the heating path in the DSC typically show several exothermic and melting peaks. Therefore, compositions that show clear melting peaks also present a number of difficulties for the correct interpretation of T_L. Some of the difficulties discussed in the literature and the use of DSC for the determination of the *liquidus* are reviewed in the following paragraphs.

The original signal from any transformation occurring in a DSC is measured with thermocouples as an electrical potential difference and processed into heat flux by the equipment's software, given the geometry and thermal properties of the sample holder. However, it is especially difficult to interpret results when simultaneous processes occur,[9] as in multicomponent glasses. A DSC peak can be characterized by its onset, maximum, and endpoint temperatures (Fig. 1). It is straightforward to obtain the maximum temperature of a DSC melting peak, while its physical meaning is not so clear. The determination of the other characteristic points—onset and endpoint temperatures—is not so straightforward. Conventionally, these last two points have been determined as the intersection of tangents to the curve, traced on the baseline and on the peak side, on the

L. Pinckney—contributing editor

Manuscript No. 27543. Received February 9, 2010; approved June 1, 2010.
This work was supported by Saint Gobain and Brazilian funding agencies FAPESP (# 2007/08179-9), CAPES, and CNPq.
Presented at the 9th International Symposium on Crystallization in Glasses and Liquids, Foz do Iguaçu, PR, Brazil, September 10–13, 2009 (Poster Session, Presentation 0389).
[†]Author to whom correspondence should be addressed. e-mail: ebferreira@sc.usp.br
[‡]Present address: Escola de Engenharia de São Carlos, Departamento de Engenharia de Materiais, Universidade de São Paulo, São Carlos 13566-590, SP, Brazil.

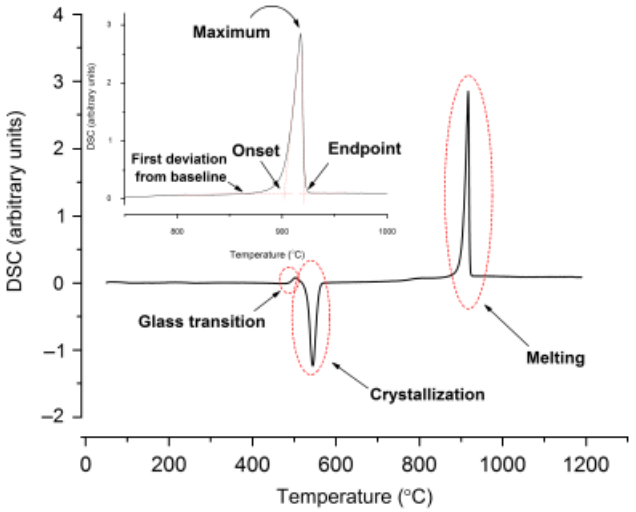

Fig. 1. Typical differential scanning calorimetry curve of a glass that crystallizes readily. The characteristic temperatures of the melting peak are shown in detail.

low- and high-temperature peak side, respectively. This method is called the "tangent method," but it is not a standard method and its uncertainty is difficult to estimate. Moreover, it is also difficult to unambiguously draw tangents on a nonstraight DSC peak side, on overlapped peaks, or on a broad or a low-intensity peak. All these factors increase the uncertainty of the tangent method.

Garidel *et al.*[10] compared the tangent method with an alternative method for the determination of the onset and endpoint temperatures of the DSC melting peak. Their method simulates the variation of heat capacity as a function of temperature, assuming that the onset and endpoint temperatures of the DSC melting peak are the *solidus* (the limiting temperature below which there are only solid phases in equilibrium) and the *liquidus*, respectively. They built binary-phase diagrams of organic compounds using the proposed technique and compared the results with those obtained by the tangent method. The resulting diagrams showed that the *liquidus* obtained from both methods were in good agreement, whereas the *solidus* deviated considerably.

Pedersen *et al.*[11] used another method to estimate the *solidus* and *liquidus* by DSC of an Sn–Pb eutectic phase diagram. They determined the onset and endpoint of DSC melting peaks at different heating rates using the tangent method. Heating rates from 0.1° to 30°C/min were used. They assumed that a fit to the data points plotted as a function of the heating rate and extrapolated to null heating rate represented the *solidus* in the case of the onset, and the *liquidus* in the case of the endpoint. For their system, they found that the onset temperature of the melting peak was independent of alloy composition and heating rate (the eutectic temperature in this case), while the endpoint temperature varied linearly with the heating rate, with almost the same slope for all compositions. The *solidus* and *liquidus* agreed within a few percent with a published phase diagram. Pedersen *et al.*[11] used several heating rates, small sample masses, and high-purity elements (Pb—99.9999% and Sn—99.999%), corroborating their method.

When melting is detected as an endothermic peak in a DSC experiment, the first shift from the baseline (see detail in Fig. 1) before the peak in the heating path, rather than the conventional onset temperature, can be considered the best estimate of the *solidus*. This can be deduced from the definition of the *solidus*—the temperature below which no liquid exists in equilibrium. Thus, the first sign of melting indicates that such temperature has been reached. In the case studied by Pedersen *et al.*,[11] this point was very close to the onset obtained by the tangent method. Nevertheless, when the DSC melting peak is too broad, the onset or endpoint temperatures determined by the tangent method may differ considerably from one another and from the first deviation from the baseline.

The construction of binary-phase diagrams of organic compounds has been aided by DSC in other works. In one of them, Young *et al.*[12] determined the *liquidus* by DSC and compared the results with the calculated *liquidus* as a function of composition, considering an ideal solid solution, knowing the latent heat of fusion of the pure component, its melting temperature, and its molar fraction in the mixture. Low heating rates were adopted to achieve near equilibrium conditions. However, the use of very low heating rates is sometimes not effective for commercial multicomponent glasses because they often do not crystallize, even after a long heat-treatment time, thus precluding the detection of the melting peak during a DSC run.

An alternative method of DSC analysis, called the stepwise method, can also be used to reach near equilibrium conditions. Charsley *et al.*[13] studied this method, also called *isothermal calibration*, whereby the temperature of the sample is raised stepwise with isothermal intervals between the steps until melting is completed. The occurrence of melting is observed as an endothermic shift from the baseline of the DSC trace determined by this method. A comparison between the *liquidus* determined by the stepwise method (taken as reference) and by extrapolation of the onset temperature determined at different rates to null heating rate led to the conclusion that the extrapolated onset temperature provided the *liquidus* at equilibrium. Onset temperatures determined by the tangent method and at heating rates of 0.5°–10°C/min were used in the second case. The use of the onset temperature was justified by the fact that pure (stoichiometric) reference-grade compounds are used. Nevertheless, similar difficulties are expected when applying either the stepwise method or the dynamic extrapolation method to complex glass-forming compositions, e.g., due to peak shape and overlap.

According to Höhne *et al.*,[14] broad melting peaks appear in DSC analyses of nonstoichiometric and noneutectic compositions. In these cases, the onset temperature corresponds to melting in the eutectic reaction, and the "subsequent broad endothermic effect is caused by the dissolution of the remaining solid component into the equilibrium melt." Thus, the endpoint temperature would correspond to the *liquidus*. On the other hand, pure or eutectic compositions "melt during a DSC run at a well-defined temperature" and this temperature is usually associated with the onset obtained by the tangent method.

From this brief review, the following conclusions can be drawn: (i) there is no standard procedure to determine T_L by DSC/DTA; and (ii) there is no consensus about the most adequate method to determine the *liquidus* using DSC/DTA, although most evidence favors the extrapolated endpoint temperature for noncongruent melting and nonstoichiometric compositions. Because the traditional procedures to measure the *liquidus* of multicomponent glasses are laborious and time consuming, an alternative procedure would be very welcome. The objective of the present study is therefore to establish a DSC method for faster and reliable determination of the liquidus of multicomponent glasses that are reluctant to crystallize.

II. Experimental Procedure

Three experimental sets were designed to achieve the above-described objective. First, to understand how composition affects the DSC melting peaks, glass samples with several compositions of a well-known binary system, Li_2O–B_2O_3, were analyzed by DSC and the results were compared with the published equilibrium phase diagram. Most of the Li_2O–B_2O_3 glasses were kindly supplied by Prof. Steve Feller of Coe College, USA. Second, to use three multicomponent glasses supplied by Saint-Gobain Recherche (SGR, Aubervilliers, France), for which the *liquidus* was previously determined, the characteristic temperatures of DSC melting peaks obtained at different heating rates were extrapolated to 0°C/min, and the resulting values compared to give the *liquidus*. Finally, a third set of experiments was designed to check the DCS *liquidus* of the SGR

glasses by the traditional procedure of heat treating in a gradient furnace and carrying out microscopy analysis.

DSC analyses were carried out in a Netzsch DSC 404 (NETZSCH-Gerätebau GmbH, Selb, Bavaria, Germany) with covered Pt pans. Powders were obtained by grinding the glasses in an agate mortar and pestle.

(1) Liquidus of Li_2O–B_2O_3 by DSC

Figure 2 shows the Li_2O–B_2O_3 phase diagram[15] indicating the compositions under study. The glass preparation procedure will be described elsewhere (S. Feller, unpublished data). Powder samples with particle sizes between 38 and 22 μm and weighing about 20 mg were analyzed by DSC, applying a heating rate of 10°C/min and using an empty pan as reference.

These DSC experiments were not repeated at different heating rates. Thus, later, to estimate the effect of the heating rate, stoichiometric monolithic glass samples of composition $Li_2O \cdot 2B_2O_3$ were analyzed by heating them at different rate and comparing the resulting DSC melting peaks. Before the DSC analysis, the samples were heat treated at 545°C for 12 h to crystallize them. DSC runs were carried out at 5°, 10°, and 20°C/min.

(2) DSC Determination of the Liquidus of Multicomponent SGR Glasses

Three multicomponent glasses that are reluctant to crystallize with *liquidus* determined previously (by the traditional method) were kindly supplied by Saint-Gobain Recherche (SGR). The designation and *liquidus* for these glasses are shown in Table I. The glasses were ground into fine powders and heat treated well below the given *liquidus* for sufficient time to promote crystallization, enabling the detection of a melting signal by DSC. Table I shows the crystallization heat treatments for each glass. The heat-treated samples were further ground into particle sizes of 22–38 μm and DSC analyses were run at heating rates of 5°, 10°, and 20°C/min. The Pt pans and sample weights were fixed.

Table I. Saint-Gobain Recherche (SGR) Glass Designations, Heat Treatment Conditions for Crystallization, and Respective *Liquidus* Informed by SGR

		Crystallization heat treatment		
Glass designation	Informed T_L (°C)	t (h)	T (°C)	Particle size (μm)
SG1	920	24	860	<22
SG2	920	48	860	<38
SG3	960	48	860	<38

The characteristic points (onset, maximum, and endpoint) of the DSC melting peaks were obtained by the tangent method.

(3) Liquidus of Multicomponent SGR Glasses Determined by the Gradient Furnace Method

The *liquidus* of the SGR glasses was also determined independently by the gradient furnace technique. Glass samples were ground into particles with sizes under 38 μm and heat treated in a regular furnace at 860°C for 48 h to obtain a material with a large crystalline fraction (the same temperature mentioned above to produce crystallization before the DSC runs). These heat-treated samples were then ground into particles between 22 and 38 μm and pressed into sample holders made of alumina tubes of 3.5 mm inner diameter and 12 mm high, approximately, supported on alumina plates. The sample holders were placed in a gradient furnace and positioned precisely under individual thermocouples in order to measure their temperatures accurately. The thermocouples were calibrated by comparing them with a Pt/Pt-13% Rh reference thermocouple at temperatures close to the gradient temperatures. The furnace produced a temperature gradient between 872° and 921°C. The samples were heated at 10°C/min, and after 24 h at the treatment

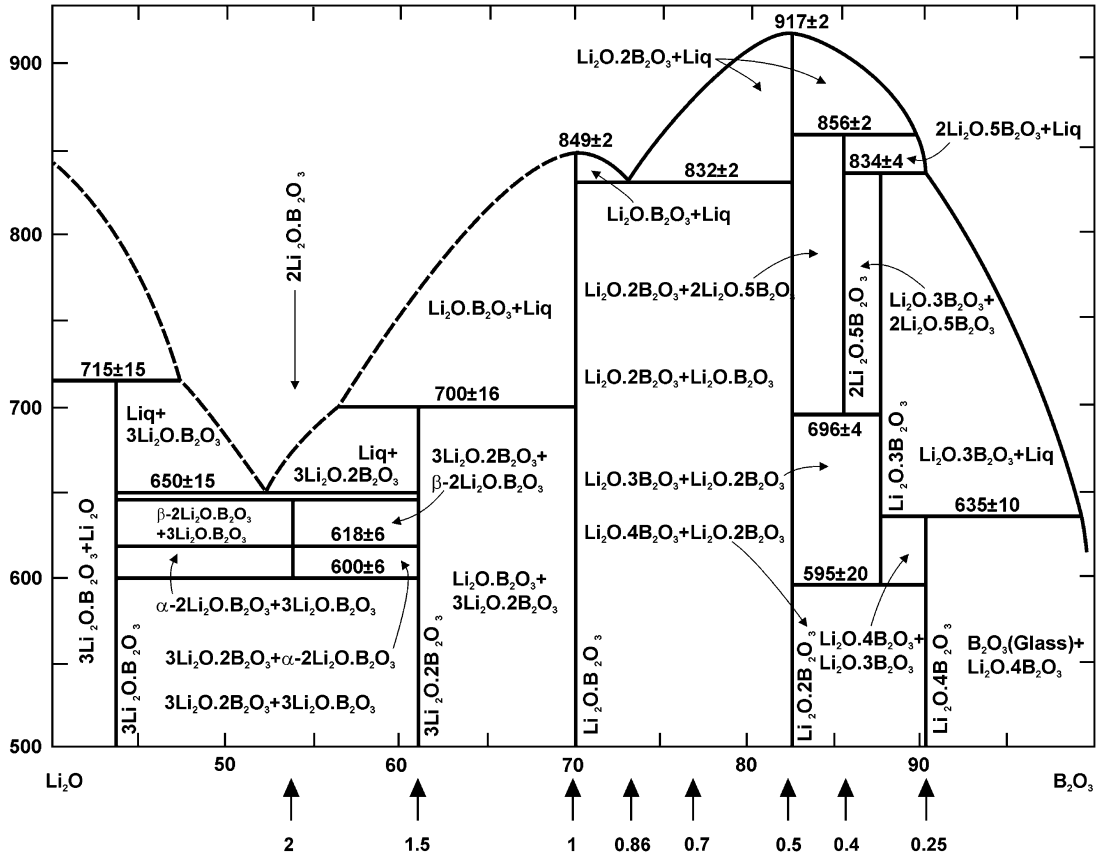

Fig. 2. Li_2O–B_2O_3 equilibrium phase diagram (wt%). The arrows indicate the Li_2O/B_2O_3 mole ratios of compositions analyzed by differential scanning calorimetry (after Sastry and Hummel[15]).

temperatures they were cooled by turning off the furnace. The periods of time on the heating or cooling path were considered not to affect the crystal fraction of the samples to any significant degree. A thin disk was later cut from each sample, polished, and analyzed by optical microscopy through transmitted polarized light, to search for crystals. A Leica DMRX optical microscope (Leica Microsystems Inc., Bannockburn, IL) was used for this task.

III. Results

Figure 3 shows the resulting DSC curves from Li_2O–B_2O_3 samples, indicating the different molar ratios. Table II compares the characteristic points of melting peaks from the DSC traces in Fig. 3 against data from the published equilibrium phase diagram[15] (Fig. 2).

Figure 3 shows that DSC traces of compositions $Li_2O/B_2O_3 = 0.25$, 0.4, 0.7, 1.5, and 2.0 have a melting peak composed of two or more overlapping peaks, or present a complex peak (i.e., broad or with a shoulder). In Table II, the uncertainty in attributing an endothermic peak for the beginning of the melt (in the traces of Fig. 3) is expressed as a sign "?" for compositions for which $Li_2O/B_2O_3 = 0.25$ and 0.40. On the other hand, the stoichiometric compositions with $Li_2O/B_2O_3 = 0.5$, and 1.0 and 0.86 (eutectic) show a sharp melting peak. Actually, the composition with $Li_2O/B_2O_3 = 0.86$ presents a shoulder on the left side of the melting peak, which is probably due to a small deviation from the nominal eutectic composition.

Figure 4 shows the DSC melting peaks of a stoichiometric $Li_2O \cdot 2B_2O_3$ glass at different heating rates. The characteristic points for each curve are indicated (the first deviation from the baseline is included for discussion). Figure 5 shows the characteristic points as a function of heating rate. The points were fit by straight lines and the corresponding equations are shown.

The extrapolations of the straight lines to 0°C/min aim to eliminate the effect of the heating rate and to estimate the characteristic temperatures at equilibrium. These values can thus, in principle, be compared with those of the equilibrium phase diagram.

There is only one observable melting peak in the DSC curves shown in Fig. 4, as would be expected for a congruent-melting compound. The temperature of first deviation from the baseline or the onset should approach the *liquidus* of the equilibrium diagram taken as reference, 917°±2°C.[13,16] However, the temperatures extrapolated to 0°C/min result in 872°C for the first deviation from the baseline, as observed in Fig. 5, and 913°C for the endpoint, a range of 41°C, which is more coherent if we admit a slight deviation of the experimental composition from the $Li_2O \cdot 2B_2O_3$ stoichiometric composition to a somewhat higher a B_2O_3 content, giving a *liquidus* below 917°±2°C. The deviation from stoichiometry can result, in this case, in a broader peak, and its endpoint would be a better measurement of *liquidus*.

Table II. Comparison of Characteristic Points of DSC Melting Peaks Against the Literature Data of Li_2O–B_2O_3 Glasses

	Onset		Endpoint			
Li_2O/B_2O_3 (mol/mol)	T_{On} (°C)†	$T_{Solidus}$ (°C)‡	T_{End} (°C)†	T_{End} corrected (°C)§	T_L (°C)‡	ΔT (°C)¶
2.00	629	650±15	676	668	673	−5
1.50	692	700±16	790	782	768	14
1.00	838	—	856	848	849±2	−3 to 1
0.86	826	832±2	846	838	832±2	4 to 8
0.70	826	832±2	889	881	879	2
0.50	908	—	926	918	917±2	−1 to 3
0.40	?	856±2	907	899	905	−6
0.25	?	635±10	837	829	834±2	−3 to −7

†From DSC experiments. ‡From the Li_2O–B_2O_3 phase equilibrium diagram[15] (Fig. 2). §T_{End} corrected = T_{End}−8°C. ¶$\Delta T = T_{End}$ corrected−T_L.

A comparison of the above endpoint, 913°C, with the endpoint of the same composition measured at 10°C/min, which is 922°C, shows a difference of 8°C. This difference thus provides an estimate for the temperature correction (effect of heating rate) to be applied to the endpoint temperatures measured in the DSC melting peaks of Fig. 3, also shown in Table II. The correct results are also shown in Table II. One can see a good agreement between the corrected endpoints and the *liquidus* from the diagram, with shifts between −7° and 14°C.

The onset temperature has been sometimes[11] related with the solidus. In this work, we compared these temperatures for Li_2O–B_2O_3 compositions. However, the onset points obtained by the tangent method for all Li_2O–B_2O_3 glasses are far from the *solidus*.

Figure 6 shows an optical micrograph of a section of a sample heat treated at 860°C for 48 h. This micrograph was obtained using the thin-section technique. The results for the SGR glasses are summarized in Table III. The endpoints plotted as a function of heating rate are shown in Fig. 7 for the three SGR glasses.

The results obtained for the SGR glasses lead to the same overall picture: the extrapolations of the endpoints to 0°C/min are within 10°C of the SGR *liquidus* measured by the simple-furnace technique.

Crystallized SG1 samples were prepared as described earlier and heat treated in a gradient furnace for 24 h. The temperature range was set to approximately the *liquidus* measured at SGR. The purpose of this procedure was to determine the *liquidus* by visually analyzing the dissolution of crystals in an optical microscope. Dissolution is normally much faster than crystal growth, which makes it easier to observe. For most glasses, the crystal growth rate at temperatures near the *liquidus* is very low (it is 0 at T_L), which hinders an accurate determination by

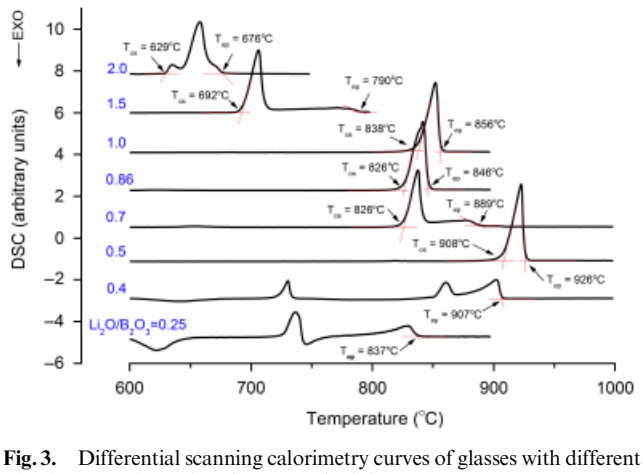

Fig. 3. Differential scanning calorimetry curves of glasses with different Li_2O/B_2O_3 molar ratios shown on the left.

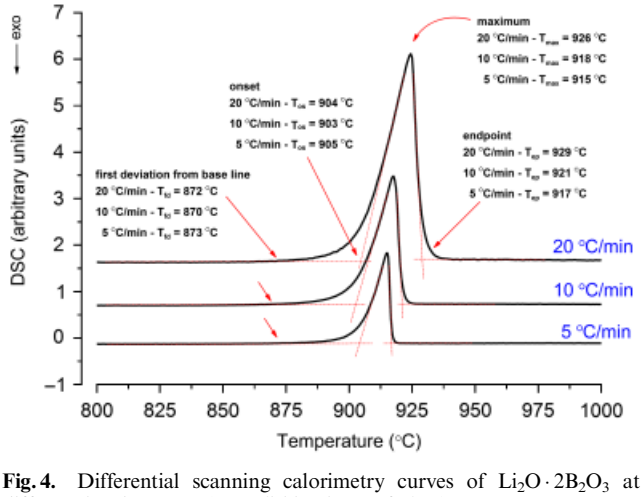

Fig. 4. Differential scanning calorimetry curves of $Li_2O \cdot 2B_2O_3$ at different heating rates (monolithic pieces of glass).

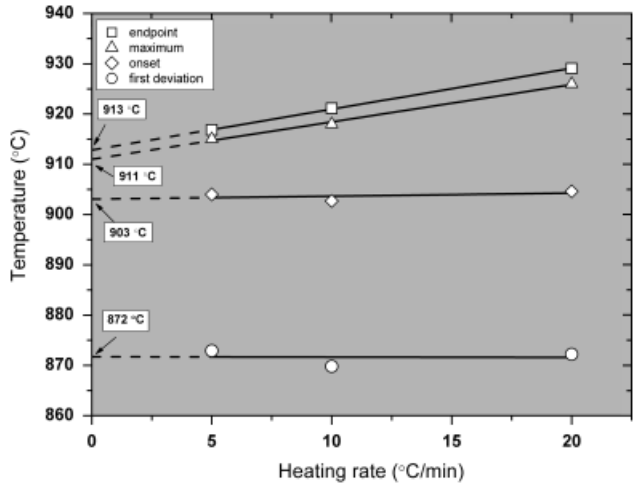

Fig. 5. Characteristic melting points versus heating rate fit by straight lines. Extrapolations to 0°C/min are shown in the boxes.

looking for crystals grown after heat treatments at these very high temperatures. On the other hand, the dissolution rate at temperatures only slightly above the *liquidus* is much higher than the crystal growth rate, which means that less time is needed to observe the total dissolution of the previously grown crystals.

The results for the SG1 glass obtained by this gradient furnace technique are shown in Fig. 8. Samples treated at temperatures below the *liquidus* must show some crystals or partially crystalline microstructures, while samples heated above the *liquidus* must remain totally glassy. The image in Fig. 8a is darker because this sample is thicker than the others, but it is possible to observe that it is intensely crystallized. Other samples were partially crystallized after treatment at temperatures from 872°C (Fig. 8a) to 918°C (Fig. 8f).

The sample treated at 921°C (Fig. 8g) showed much weaker signs of crystals, if at all, indicating a *liquidus* between 918° and 921°C, or at least slightly higher than 921°C, which is very close to the *liquidus* determined by SGR (920°C) and that obtained by DSC (930°C).

The microstructure shown in Fig. 8h corresponds to the same sample of Fig. 8g, but at the interface with the crucible. A glass layer located around the inner wall of the crucible was observed in all samples as seen in Figs. 8(d) and (h) (the thin section of the Al_2O_3 crucible appears in black in the bottom of these figures). Probably, these regions are more difficult to crystallize than the glassy interior due to an increase of Al_2O_3 in the glass composition caused by chemical dissolution of the crucible by the molten glass. We believe that the crystals shown in Fig. 8h, growing from the glassy film next to the crucible wall inwards the bulk glass, are due to this compositional wall effect.

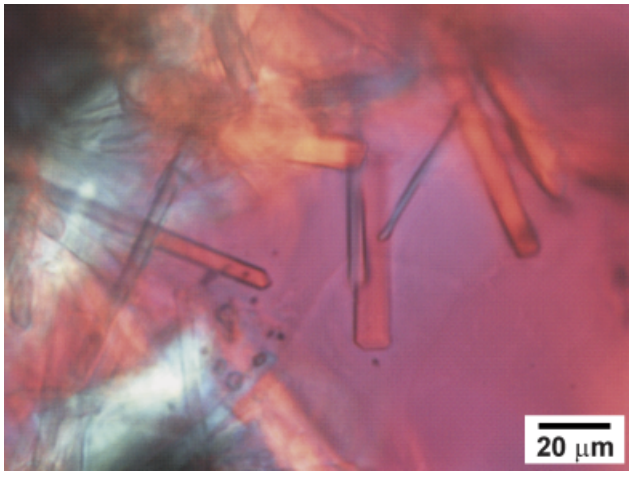

Fig. 6. Microstructure of the initial SG1 sample after heat treatment at 860°C for 48 h. Crystals are clearly visible.

Table III. Results of Saint-Gobain Recherche (SGR) Commercial Glasses

Glass	Characteristic points (°C)	Heating rate (°C/min) 5	10	20	Extrapolation at 0°C/min	Liquidus by SGR (°C)
SG1	T_{On}	732	764	798	715	920
	T_{Max}	903	901	902	902	
	T_{End}	933	937	944	932	
SG2	T_{On}	776	786	804	767	920
	T_{Max}	886	895	905	881	
	T_{End}	924	932	958	910	
SG3	T_{On}	—	—	—		960
	T_{Max}	—	—	—		
	T_{End}	995	1040	1090	970	

The conclusion that the *liquidus* temperature is between 918° and 921°C (or slight above 921°C) is made based in the very glassy appearance (i.e., the previous crystals were totally dissolved during the heat treatment) of the interior of the sample in Fig. 8g.

IV. Discussion

During a DSC run of easily crystallizable compositions that melt congruently (such as $Li_2O \cdot 2B_2O_3$), the glass readily crystallizes after the glass transition and the resulting crystals should melt with a well-defined peak in the DSC. Even for these compositions, however, the DSC melting peak has a finite width due to equipment inertia. The detection of the temperature at which the studied phenomenon begins depends on the reaction kinetics and also on the thermal conductivity and heat capacitance of the sample, reference, and sample holder. Thus, an increase of the heating rate shifts the melting peak toward higher temperatures. However, if the melting peak is sharp, its onset, maximum, and endpoint temperatures should not differ much.

In the literature,[11] most DSC melting peaks of metallic compounds that melt congruently are sufficiently sharp that no significant difference between onset, maximum, and endpoint can be observed. However, in our experiments, even with glasses of almost stoichiometric composition (Fig. 4, $Li_2O \cdot 2B_2O_3$), the DSC melting peaks are somewhat broadened. This could be justified by the high heating rates, low thermal conductivity, and sample masses used, or by some deviation in the composition from the exact stoichiometry.

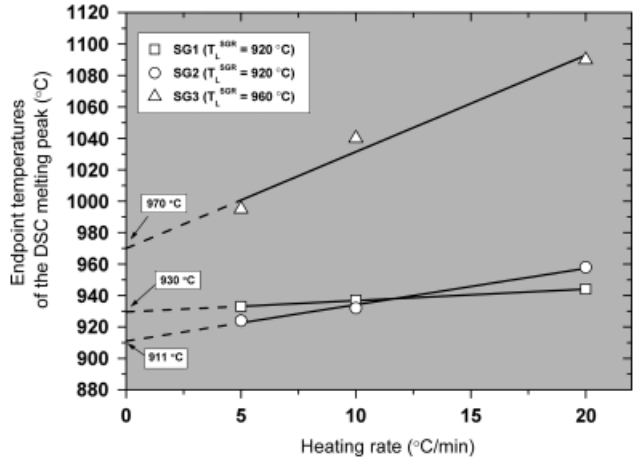

Fig. 7. Differential scanning calorimetry endpoints of Saint-Gobain Recherche (SGR) glasses extrapolated to 0°C/min (in the boxes), which are in reasonable agreement with the *liquidus* determined by SGR by the simple furnace technique (T_L^{SGR}, indicated in the legend).

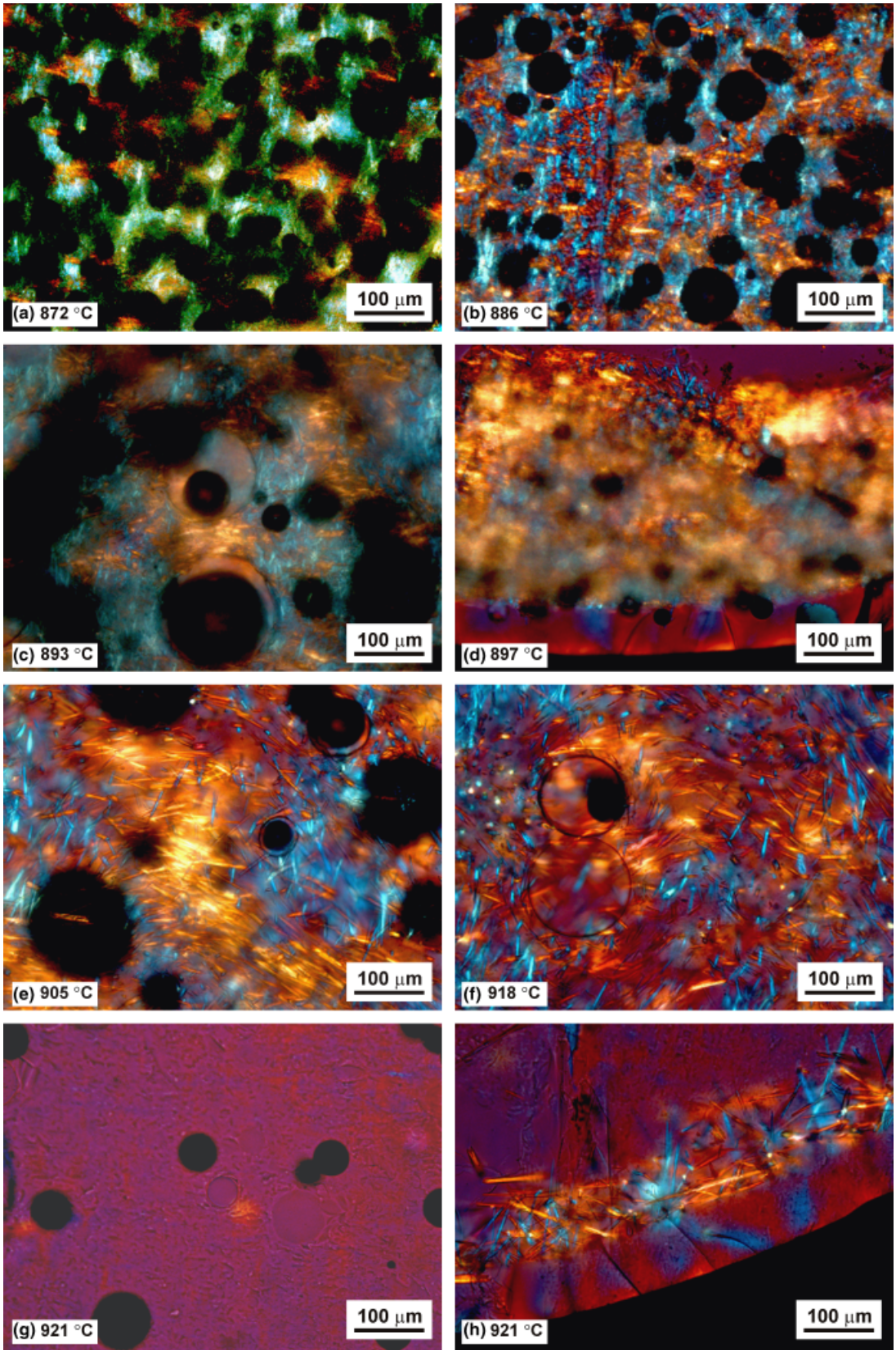

Fig. 8. (a–g): SG1 glass samples treated in a gradient furnace for 24 h at the indicated temperatures. Thin sections of the samples under polarized transmitted light. The yellow and blue needles are crystals, the circular dark objects are trapped bubbles during sintering of the glass powder, and the magenta background is glass (colored in the online version). (h) Interface sample/crucible of (g). See text for details (colored in the online version).

The beginning of the melting peaks obtained for these glasses (Fig. 4), i.e., the point at which the DSC curve begins to deviate from the baseline, was about 872°C for the tested $Li_2O \cdot 2B_2O_3$ samples, but it is difficult to accurately determine this point. However, any deviations from the nominal composition of the samples would produce reactions starting at 832° or 856°C (the *solidus* for adjacent compositions—Fig. 2).

Based on the fact that the melting behavior is intrinsically related to the crystallized structure, the shape of the melting peak in the DSC curves of glasses can be explained by the possible formation of nonequilibrium phases during dynamic crystallization, with lower *liquidus* than the equilibrium phases (dynamic crystallization can favor the formation of nonequilibrium phases). Glass inhomogeneity is another important factor in the formation of unexpected phases, but was not analyzed in this work.

A comparison of the melting peaks in the DSC heating paths for the stoichiometric $Li_2O \cdot 2B_2O_3$ glass heat treated previously for crystallization indicates the absence of any major differences. Thus, at least for this composition, dynamic crystallization had no effect on the DSC melting peak.

The use of the extrapolated endpoint to null heating rate yielded results that are in agreement with the equilibrium phase diagram and motivated the use of the same procedure for complex multicomponent glasses.

The analysis of nonstoichiometric or incongruently melting compositions is different from that applied to stoichiometric systems. The melting of such compositions (after previous crystallization) is not punctual and, on the heating path, crystals should coexist with the surrounding liquid, from the *solidus* up to the end of the process, which occurs in a certain temperature range. During nonisothermal melting in a DSC experiment, the temperature at which the last crystals dissolve should be the *liquidus*, but due to the finite heating rates used, some overestimate can occur due to limited thermal conductivity of the sample and overall equipment inertia. Therefore, a good estimate for this temperature is the endpoint of the melting peak.

The reaction rate at the melting point (for congruently melting composition) or in the melting range (for incongruent melting or nonstoichiometric compositions) depends on the heating rate used in the experiment. If the heating rate in the DSC is high, due to the limited thermal conductivity in the device, the heat signal detected by the equipment can be at a higher temperature than that at which the crystals actually melted. DSC peaks associated with endothermic or exothermic reactions are rate dependent. In the present work, the melting peaks are linearly displaced to higher temperatures for relatively high heating rates (5°, 10°, and 20°C/min). In addition, many authors[11,13,17] have observed a linear shift of the onset of DSC melting peaks with heating rate down to very low rates (0.1°C/min). Pedersen *et al.*,[11] particularly, observed it in a wide range (0.1°–30°C/min). The combined results of these studies suggest that the extrapolation of the endpoint follows a linear relationship with any heating rate from high to null rate and can provide an estimate of the *liquidus* of multicomponent glasses [the temperature at which the last crystal would dissolve at 0°C/min (isothermal condition)]. However, we point out that the validity of a perfectly linear relationship of the peak position with heating rate over such a wide range of rates down to zero rate must still be checked in future works.

The main difference observed between the melting peaks of simple and complex glasses is the high temperature side of the melting peak after the maximum. The melting peaks of stoichiometric glasses are asymmetric and, after the maximum, there is an abrupt fall of the DSC signal toward the baseline. In contrast, in multicomponent, nonstoichiometric glasses, after the maximum, the DSC signal does not drop abruptly; instead, it slowly declines toward the baseline. This behavior of nonisothermal analyses of multicomponent glasses can be explained by the continuous melting of crystals during the final part, which widens the DSC melting peak. The fraction of such crystals melting at each step of temperature increase is low and thus their signal is low, accumulating until the last crystal finally melts.

V. Conclusions

The *liquidus* is an equilibrium temperature; hence, to properly measure it, the equilibrium phases must be present in the sample. Therefore, for multicomponent glasses that do not crystallize during a DSC run, a previous heat treatment is necessary in order to reach close-to-equilibrium conditions. The endpoint of the DSC melting peaks measured at different heating rates and extrapolated to 0°C/min was the best estimate of the *liquidus* of such glasses. In this way, we found a good agreement (most results differ by not >10°C) for the results of three methods used to determine the *liquidus* of multicomponent glasses.

We, therefore, developed and successfully tested a DSC method to estimate the *liquidus* of reluctant-to-crystallize, good glass-forming systems. Because of the small amount of glass needed, the possibility of instrumental (computer aided) detection, the simultaneous crystallization pretreatment of many different compositions, and the speed of the DSC analysis developed in this work, this technique is a very useful alternative to estimate the *liquidus* of simple or multicomponent glasses. The proposed nonisothermal technique is very useful for screening glass compositions.

Acknowledgments

We are indebted to Drs. Herve Arribart and Cecille Jusseaume of SGR, France, and Prof. Steve Feller, Coe College, USA, for providing samples, encouragement, and very useful suggestions for this study. Thanks are also due to Luis Felipe Vendramim for conducting some experiments, to Dr. Oscar Peitl, LaMaV-UFSCar, for helping with the gradient furnace, and to Dr. Vladimir Fokin, Russia, for his invaluable suggestions and discussions.

References

[1]J. D. Vienna, P. Hrma, J. V. Crum, and M. Mika, "Liquidus-Temperature Model for Multi-Component Glasses in Fe, Cr, Ni and Mn Spinel Primary Phase Field," *J. Non-Cryst. Solids*, **292** [1–3] 1–24 (2001).

[2]Q. Rao, G. F. Piepel, P. Hrma, and J. V. Crum, "Liquidus Temperature of HLW Glasses with Zirconium-Containing Primary Crystalline Phases," *J. Non-Cryst. Solids*, **220** [1] 17–29 (1997).

[3]C. Dreyfus and G. Dreyfus, "A Machine Learning … Approach to the Estimation of Liquidus Temperature of Glass-Forming Oxides Blends," *J. Non-Cryst. Solids*, **318** [1–2] 63–78 (2003).

[4]V. N. Makanov, I. V. Makarova, O. V. Suvorova, and A. N. Sakharchenko, "Programming and Calculation of Process Parameters in Production of Silicate Materials," *Glass Ceram.*, **59** [3–4] 80–3 (2002).

[5]R. G. C. Beerkens and R. Conradt, "Round Robin Test on Liquidus Temperature of Soda–Lime–Magnesia–Silica Float Glass Samples," *Glass Tech.: Eur. J. Glass Sci. Technol. A*, **49** [5] 205–12 (2008).

[6]L. Wondraczek and L. Beunet, "Liquidus Prediction in Multicomponent Lithium Alumosilicate Glasses," *J. Am. Ceram. Soc.*, **91** [4] 1309–11 (2008).

[7]A. Fluegel, "Modeling of Glass Liquidus Temperatures using Disconnected Peak Functions"; Presentation at ACerS 2007 Glass and Optical Materials Division Meeting, Rochester, NY, USA.

[8]A. Fluegel, *Glass Liquidus Temperature Calculation.* Available at http://glassproperties.com/liquidus/ (accessed February 1, 2010).

[9]E. Verdonk, K. Schaap, and L. C. Thomas, "A Discussion of the Principles and Applications of Modulated Temperature DSC (MTDSC)," *Int. J. Pharm.*, **192** [1] 3–20 (1999).

[10]P. Garidel, C. Johann, and A. Blume, "The Calculation of Heat Capacity Curves and Phase Diagrams Based on Regular Solution Theory," *J. Therm. Anal. Calorim.*, **82** [2] 447–55 (2005).

[11]A. S. Pedersen, N. Pryds, S. Linderoth, P. H. Larsen, and J. Kjoller, "The Determination of Dynamic and Equilibrium Solid/Liquid Transformation Data for Sn–Pb Using DSC," *J. Therm. Anal. Calorim.*, **64** [3] 887–94 (2001).

[12]P. H. Young, D. Dollimore, and C. A. Schall, "Thermal Analysis of Solid–Solid Interactions in Binary Mixtures of Alkylcyclohexanes using DSC," *J. Therm. Anal. Calorim.*, **62** [1] 163–75 (2000).

[13]E. L. Charsley, P. G. Laye, V. Palalollu, J. J. Rooney, and B. Joseph, "DSC Studies on Organic Melting Temperature Standards," *Thermochim. Acta*, **446** [1–2] 29–32 (2006).

[14]G. W. H. Höhne, W. Hemminger, and H. J. Flammersheim, *Differential Scanning Calorimetry—An Introduction for Practitioners*. Springer Verlag, Berlin, 1996.

[15]B. S. R. Sastry and F. A. Hummel, "Studies in Lithium Oxide Systems. V. Li_2O–$Li_2O \cdot B_2O_3$," *J. Am. Ceram. Soc.*, **42** [5] 216–8 (1959).

[16]A. N. Sembira and J. G. Dunn, "High Temperature Calibration of DTA and DSC Apparatus Using Encapsulated Samples," *Thermochim. Acta*, **274**, 113–24 (1996).

[17]D. E. G. Jones, R. Wang, and A. M. Turcotte, "The Effect of Pressure and Heating Rate on the Melting Behavior of Indium and Tin," *Can. J. Chem.*, **84**, 407–11 (2006). □